ACS APPLIED MATERIALS & INTERFACES

Research Article

www.acsami.org

Photochemically Reversible Liquefaction and Solidification of Multiazobenzene Sugar-Alcohol Derivatives and Application to Reworkable Adhesives

Haruhisa Akiyama,*[,†] Satoshi Kanazawa,[†] Yoko Okuyama,[†] Masaru Yoshida,[†] Hideyuki Kihara,[†] Hideki Nagai,[‡] Yasuo Norikane,[§] and Reiko Azumi[§]

[†]Nanosystem Research Institute, National Institute of Advanced Industrial Science and Technology (AIST), Central 5, 1-1-1 Higashi, Tsukuba, Ibaraki 305-8565, Japan

[‡]Research Institute of Instrumentation Frontier, National Institute of Advanced Industrial Science and Technology (AIST), Central 2, 1-1-1 Umezono, Tsukuba, Ibaraki 305-8568, Japan

[§]Electronics and Photonics Research Institute, National Institute of Advanced Industrial Science and Technology (AIST), Central 5, 1-1-1 Higashi, Tsukuba, Ibaraki 305-8565, Japan

Supporting Information

ABSTRACT: Multiazobenzene compounds, hexakis-*O*-[4-(phenylazo)-phenoxyalkylcarboxyl]-D-mannitols and hexakis-*O*-[4-(4-hexylphenylazo)-phenoxyalkylcarboxyl]-D-mannitols, exhibit photochemically reversible liquefaction and solidification at room temperature. Their photochemical and thermal phase transitions were investigated in detail through thermal analysis, absorption spectroscopy, and dynamic viscoelasticity measurements, and were compared with those of other sugar-alcohol derivatives. Tensile shear strength tests were performed to determine the adhesions of the compounds sandwiched between two glass slides to determine whether the compounds were suitable for application as adhesives. The adhesions were varied by alternately irradiating the compounds with ultraviolet and visible light to photoinduce phase transitions. The azobenzene hexyl tails, lengths of the methylene spacers, and differences in the sugar-alcohol structures affected the photoresponsive properties of the compounds.

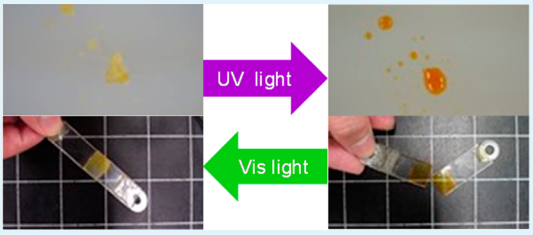

KEYWORDS: *phase transition, azobenzene, photoisomerization, reversible adhesion, liquid crystalline glass*

INTRODUCTION

Ultraviolet (UV)- or visible-light-curable resins are widely used as adhesives, printing inks, and coating and repairing materials. Adhesives that are initially liquid are solidified through irreversible photo-cross-linking and photopolymerization. This means that objects are permanently bonded together when such adhesives are cured, because the photo-cross-linking and photopolymerization cannot be reversed. Curable resins showing photoreversibility will significantly contribute to the development of resource-saving technology because the recyclable components could be readily removed from used products. Moreover, photocontrollable adhesives or coatings would enable the heat-free assembly of reworkable components during device production, resulting in efficient, sophisticated methods of manufacturing. Thus, several materials have been and are currently being studied to achieve controllable or releasable adhesion.[1−14] We have recently demonstrated how compounds with multiple azobenzene arms and a sugar-alcohol scaffold could be used as adhesives by irradiating the compounds with light to fix and unfix two glass slides. The materials showed unusual photoinduced liquefaction and solidification at room temperature, enabling completely reversible adhesion.[15] Although the photochemically induced liquid-crystalline-to-isotropic phase transitions,[16−19] two-dimensional changes in fluidity,[20,21] and sol−gel transitions[22−41] have previously been reported for azobenzene derivatives, the single-component liquid-to-solid transition at room temperature has rarely been reported. Viscoelasticity measurements performed using an atomic force scanning microscope[42,43] near the surfaces of azopolymer films have revealed that the films photofluidize during the formation of photoinduced surface-relief gratings.[44,45] The softening and fluidization of azopolymers are believed to originate from repeated light-induced trans−cis−trans isomerizations. In contrast to polymers, single crystals usually are inadequate for the isomerization of azobenzenes because they contain less free volume, which inhibits isomerization.[46−48] There have been only a few examples to date of photoinduced crystal-to-liquid transition even in photochromic dyes other than azobenzenes. The surfaces of diarylethene derivatives have shown reversible photoinduced liquid-to-crystal transitions slightly above room temperature.[49,50] Photoinduced "melting"[51] and three-phase

Received: March 2, 2014
Accepted: May 1, 2014
Published: May 12, 2014

   dx.doi.org/10.1021/am501227y | ACS Appl. Mater. Interfaces 2014, 6, 7933−7941

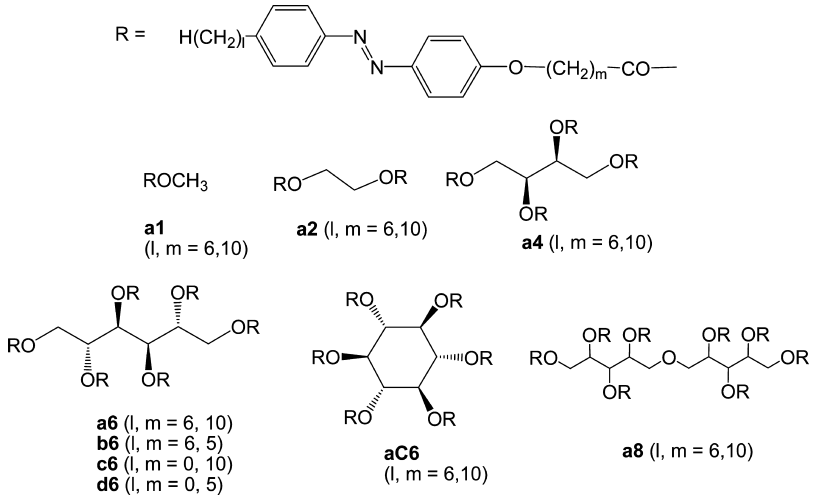

Figure 1. Chemical structures of azo-arm compounds.

(i.e., crystal−liquid−crystal) transition have previously been reported for crystalline cyclic azobenzene,[52] and photoinduced liquefaction has previously been reported for monoazobenzene prepared with a flexible chain.[53] Although we previously irradiated sugar-alcohol-scaffold-containing multiazobenzene compounds with light to demonstrate that the compounds showed reversible liquefaction and solidification, the solids were not single-crystalline but a liquid crystalline glass or another ordered phase.[15] The reversible phase transition enables the development of photocontrollable reworkable adhesives. The mechanism for the reversible liquefaction and solidification is possibly related to the photoinduced changes in molecular shape. For example, a cis unsaturated fatty acid, oleic acid (*cis*-9-octadekenoic acid; MP = 16 °C), has a lower melting point than its corresponding isomer, elaidic acid (*trans*-9-octadekenoic acid; MP = 45 °C). In other words, the bent cis isomer is a liquid, but the linear trans isomer is a solid at room temperature despite showing the same chemical composition. We have already shown that the number of azo arms on multiazobenzene compounds determines whether irradiating sugar-alcohol-scaffold-containing multiazobenzene compounds with light will photoinduce them to liquefy and solidify; for example, monomers and dimers do not exhibit photoinduced phase transition, while tetramers, hexamers, and octamers do. Therefore, multiazobenzene structures could enhance the effect of the trans−cis structural change. We prepared various compounds with and without alkyl chains and a cyclic sugar-alcohol scaffold (Figure 1) and used them as adhesives sandwiched between glass slides to further investigate how the chemical structures affected the dynamic viscoelasticities and adhesions. We previously used the compounds to bond together two glass slides, which we manually separated to preliminarily investigate the adhesions of the compounds. Here, we used a tensile shear strength tester to accurately measure the adhesions of the compounds pulled at 0.2 mm min^{-1}. In addition, we previously determined, based on the changes in the material shapes, whether the liquid or solid materials were stable. Herein, we used a rheometer to measure the storage elastic modulus (G') and loss elastic modulus (G'') of the materials and quantitatively compared the corresponding moduli for each material.

RESULTS AND DISCUSSION

Thermal Behavior of Phases. The thermal properties of the hexyl-tail-containing azo-arm compounds **a1**, **a2**, **a4**, **a6**, **a8**, **aC6**, and **b6**, have previously been reported.[54] The results of the differential scanning calorimetry (DSC) analysis performed by rapidly cooling molten **a6** from >120 °C to room temperature revealed that the **a6** film was a liquid crystalline glass (T_g = 80 °C) at room temperature. The film exhibited weak reflection color, which can be derived from the chiral liquid crystalline structure. The liquid crystalline phases could be smectic-C* and -F(I)*, although they were previously identified as smectic-A and-B.[54] Samples of **a6** were put into liquid crystalline cells to be aligned homogeneously and homeotropically for liquid crystalline phase identification. However, we could not align them in any particular direction at any temperature, which is common for the smectic-C phase; thus, we reconsidered our previous phase identification of **a6**, as shown in Table 1. The compound, **a6,** had previously been purified using column chromatography, and the solution was then evaporated to produce a powdered solid, which can be different from liquid crystalline glass. Powder X-ray diffractometry (XRD) revealed that the initial solid powders were crystalline. Hence, the liquefaction previously reported for solid **a6** corresponds to a crystal-to-liquid transition. The **a4** and **a8** liquid crystalline textures were carefully reobserved. The texture of **a4** was similar to that of **a6** just below the isotropic temperature and gradually became nonflowable, and the **a4** appeared dark during polarized optical microscopy (POM) observation. We first believed the smectic-B phase was homeotropically aligned, but the conoscopic observation revealed that it was actually an isotropic solid-like phase.

The DSC curves for the two compounds synthesized without tails, **c6** and **d6**, showed two transitions when the compounds were cooled from their isotropic phases to room temperature. The corresponding XRD spectra showed peaks attributed to the smectic liquid crystalline phase. The XRD spectrum generated for **d6** just after the first transition at 79.9 °C showed a sharp peak at 20.2 Å in the small-angle region, corresponding to the **d6** molecular length half layer, and a halo, slightly sharper than that for the isotropic phase, at ∼4.2 Å in the larger-angle region. The two glass slides sandwiching the sample actually became fixed under the shear stress applied in this temperature range, indicating that the **d6** was either highly

Table 1. Thermal Phase Behaviors of Azobenzenes

	alcohol	cooling rate (°C mm^{-1})	transition temperature (°C)	layer distance (nm) [temp (°C)]
a1[a]	methanol		Iso 65 Cr (Cr 72 Iso)	
a2[a]	ethylene glycol	2	Iso 104 Cr	
a4[b]	L-threitol	5	Iso 98 SmC* 87 SmF(I) 79 SmX	3.14 [RT], 3.14 [100]
		2	Iso 100 SmC* 96 Cr	
a6[b]	D-mannitol	5	Iso 107 SmC* 84 SmF(I)	3.06 [105], 3.11 [80]
		2	Iso 109 SmC* 86 SmF(I)	
aC6[a]	*scyllo*-inositol	2	Iso 162 Cr (Cr 171 Iso)	
a8[b]	xylitol dimer	2	Iso 113 SmA-SmC* 85 SmF(I)	3.13 [105], 3.08 [RT]
		(heating)	(SmF(I) 87 SmC*−SmA 114 Iso)	
b6[b]	D-mannitol	2	Iso 118 SmC 59 Sm F(I)	4.73 [80], 4.73 [40]
		(heating)	(Sm F(I) 61 Sm C 121 Iso)	
c6	D-mannitol	2	Iso 96 SmA 55 SmB	2.76, 1.38 [90]
d6	D-mannitol	2	Iso 80 SmA 52 SmB	2.02 [70], 2.04 [40]
		(heating)	(SmB 54 SmA 85 Iso)	

[a]Phase behaviors of these compounds were reported in the previous paper.[54] [b]Phase behaviors of these compounds were reassigned.

viscous or solid-like. Although this pattern is usually identified as fluidic smectic-A, **d6** is nonflowable. Therefore, it can be identified as an intermediate between the smectic-A and nonflowable smectic-B phases. Cooling the **d6** below the second transition at 51.5 °C further sharpened the peak at 4.2 Å in the wide-angle region, corresponding to a typical smectic-B phase. Similar phase transitions were observed at 54 and 85 °C when **d6** was heated, indicating that the **d6** liquid crystals are enantiotropic. The XRD spectra for the compound produced with longer spacers, **c6**, showed two sharp peaks at 27 and 13 Å just after the first transition at 96 °C, corresponding to the half- and quarter- molecular lengths of **c6**, respectively. Although this fluidic phase could be smectic-A, the interlayer distance is unusual. The peak at 13 Å is somewhat more intense than the one at 27 Å, so the latter does not represent the secondary diffraction, and two different layer structures could exist. The XRD pattern for **c6** cooled just above the second transition at 55 °C showed peaks attributed to crystalline **c6**, indicating that the smectic-A phase, which formed after the first transition at 96 °C, was unstable. Both ends of these materials were terminated with nonalkylated phenyl groups. Sugar-alcohol-scaffold-containing multiarm-structures significantly enhance the liquid crystallinity of even such rigid terminal compounds owing to the decreased crystallinity of the azo-arm moieties tethered to the scaffolds; the multiarm structure restricts the ability of the moieties to rearrange into a highly ordered phase.

In contrast to the linear scaffold materials, the cyclic scaffold one, **aC6**, did not exhibit any liquid crystalline phases. The DSC curves generated for the heating and cooling **aC6** showed only one obvious transition peak and one small shoulder peak.

Photoinduced Liquefaction and Solidification. Azobenzene forms thermodynamically stable trans and metastable cis isomers. Most trans azobenzene isomers transform into *cis* ones in solution irradiated with UV light, and the generated cis isomers gradually revert to trans ones at room temperature in the dark within a few days, or immediately transform into the trans-rich state on irradiation with visible light. We have already described phase transition behaviors of **a1**, **a2**, **a4**, **a6**, and **a8**.[15] Here, we show representative color pictures to clarify the difference in color and morphology changes among these compounds. The **a2** solid color and shape did not change when the **a2** was irradiated with UV light, implying that the solid did not show any photoreactivity (Figure 2). It means that the

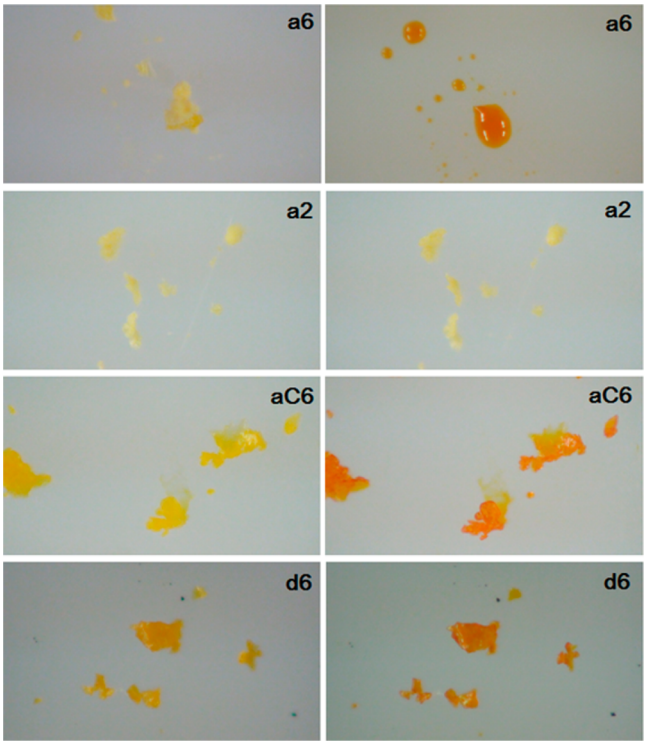

Figure 2. Photographs (1.3 × 0.72 mm) of **a6**, **a2**, **aC6**, and **d6** before (left) and after irradiation with 365 nm-light at 40 mW cm^{-2} for 1 h (right).

crystals of **a2** include no free volume for isomerization. The yellow **b6** and **a*N*** (*N* = 4, 6, and 8) solids, on the other hand, transformed into orange liquid droplets when the materials were irradiated with UV light (Figure 2). The change in color corresponds to the isomerization-induced chromatic change or disaggregation of azobenzene dyes. The *cis*-rich **b6** and **a*N*** (*N* = 4, 6, and 8) liquids were stable for several hours at room temperature, but gradually became sticky, and turned into solid after 2 days. The yellow cyclic-scaffold-containing solid, **aC6**, changed to orange but remained solid (Figure 2). The change in color suggests that the solid undergoes trans-to-cis isomerization. These results indicate that the trans- and cis-rich **aC6** solids are both stable. The two yellow, tailless compounds, **c6** and **d6**, became orange when irradiated with UV light; however, **c6** transformed into liquid droplets while **d6** remained solid.

The materials irradiated with UV light were subsequently irradiated with visible light to determine whether the phase transformations were photoreversible. The orange **d6** and **aC6**

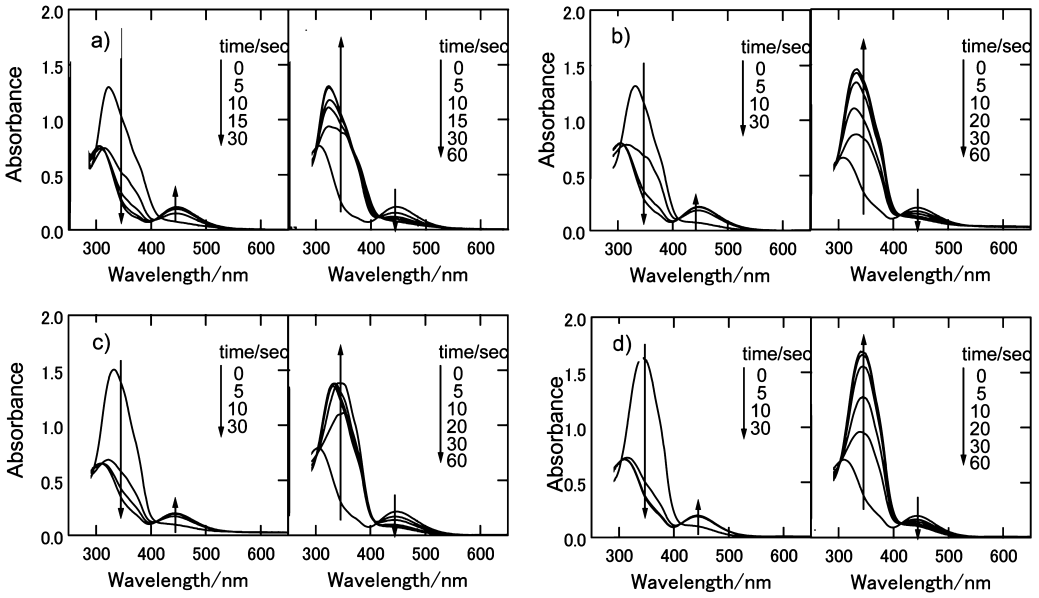

Figure 3. UV−vis absorption spectral changes of thin films of (a) **a6**, (b) **b6**, (c) **c6**, and (d) **d6** during irradiation with UV light at 40 mW cm^{-2} (left) and visible light at 25 mW cm^{-2} (right).

solids reverted to yellow ones. The orange **a*N*** (N = 4, 6, and 8) and **c6** droplets were transformed into yellow semispherical nonfluidic substances, which retained their shape when a microspatula was used to lift them from poly(tetrafluoroethylene) sheets. These results indicate that the chemical structures affected the photoinduced liquefaction and solidification.

Photoisomerization Behavior. Solutions of **a6**, **b6**, **c6**, and **d6** containing a polystyrene additive were spin-coated onto glass plates, producing ultrathin films to measure the solid-state photochemistry of the phase-changing materials. The preliminary experiment—in which solutions not containing any polymer additive were spin coated—failed to generate transparent films due to formation of island structures. Adding 5% polystyrene stabilized the solutions and produced smooth, sufficiently thin films whose absorbances were below 2 for all over the measured wavelength region(Figure 3). The $\pi-\pi^*$ transition absorption bands for the resultant **a6** films became sharper and shifted to shorter wavelengths than those for the **a6** solution (Table 2), indicating the contribution of H-aggregation of azobenzenes. The spectra for monomeric azobenzene were recovered by heating the films above their melting point. The spectra for the isotropic liquid simultaneously showed more intense absorption. The weak absorption band at 365 nm in the spectra for the unheated films indicates advantageous condensed system photochemistry because actinic light can penetrate deeper into the films. Otherwise, the strong-absorption-induced inner filter effect might limit the photoreaction near the film surface. The spectrum for the **b6** film showed similar sharp and shifted absorption bands, meaning that the azobenzenes aggregates. In contrast, the $\pi-\pi^*$ absorption band for the **c6** film did not remarkably shift and sharpen. Furthermore, the absorption band for the **d6** solid film was almost same as that for the isotropic liquid. For example, the change in the absorption spectrum for **d6** shows an isosbestic point, indicating that even the solid films contain monomeric azobenzenes. The **a6** and **b6** films also showed different spacer-length-dependent photochemical behaviors. The **b6** film showed temporal monomeric species, whose absorption maxima were at longer wavelengths, more clearly than the **a6** film while the *cis*-azobenzene was photoisomerized to *trans*-azobenzene. These results indicate a tendency for the shorterspacers to inhibit azobenzene moiety aggregation more effectively than the longer ones do. The hypsochromic shift observed for the hexylazobenzene derivatives suggests that the tail groups facilitate the H-aggregation of azobenzene moieties in the films. Isomerization ratios at photo stationary states (irradiation; 365 and 525 nm-lights) were estimated by the absorption spectra of the films of pure compounds based on the conventional manner.[55] To eliminate the influences of the orientation and aggregation of azobenzene moieties in the solid films, we dissolved the samples into chloroform after irradiation and calculated the ratios of *cis* isomers from the absorption of the solution samples (see detailed procedure in Supporting Information). The cis isomer ratios of **a6**, **b6**, and **c6** at the photostationary states are quite similar to each other (Table 3). More than 94% of trans isomers smoothly changed to *cis* isomer on irradiation with 365 nm-light, and regenerated on

Table 2. Absorption Maxima and Molar Coefficient of Azobenezenes in Chloroform Solutions

	λ_{max} (nm)	ε (L mol^{-1} cm^{-1})
a6	353	1.57×10^5
b6	352	1.63×10^5
c6	348	1.56×10^5
d6	348	1.63×10^5

Table 3. Cis Isomer Ratios at Photostationary State in Films

	cis isomer ratios (%)	
	365 nm-light	525 nm-light
a6	94.5	2.7
b6	95.2	2.6
c6	95.4	2.9
d6	88.6	5.3

dx.doi.org/10.1021/am501227y | ACS Appl. Mater. Interfaces 2014, 6, 7933−7941

irradiation with 525 nm-light. On the contrary, in the films of **d6**, the isomerization of azobenzene was significantly restricted on both irradiation conditions.The similar inactivation of isomerizability of azobenzene has been observed in glassy polymeric films.[55] Among these four azo-compounds, only the **d6** did not liquefy on irradiation. Therefore, the apparent difference in isomerization ratios implies that the isomerization of the azobenzene moieties in **a6**, **b6**, and **c6** can freely proceed through liquid phase but isomerization in **d6** was limited in glassy solid phase.

Dynamic Viscoelasticity. Measuring dynamic viscoelasticity simultaneously reveals the storage and loss elastic moduli (G' and G'', respectively) of materials. G' is always > G'' for solids and always < G'' for liquids. Hence, we measured the elastic moduli while 12 mm-diameter, 0.1 mm-thick **a6**, **b6**, **c6**, and **d6** samples gradually cooled from their isotropic phases to room temperature to determine whether the compounds were solid or liquid (Figure 4). G'' was at least five times > G' for all

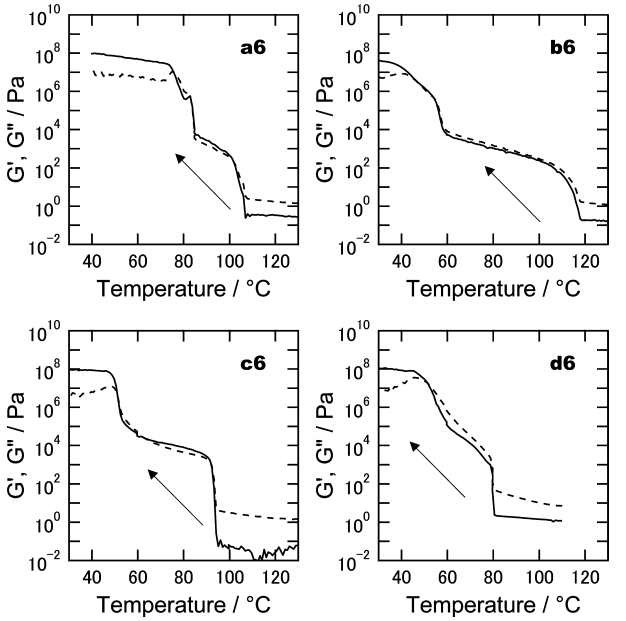

Figure 4. Dependence of storage modulus, G' (solid line), and loss modulus, G'' (dashed line), on temperature during cooling of **a6**, **b6**, **c6**, and **d6**.

the compounds above their isotropic temperatures. G'' < 5 Pa for all the compounds, which is typical for liquids. G' increased by >100-fold independent of the cooling **a6**, **b6**, and **c6** compounds at the first transition temperature and then leveled off at a magnitude comparable to that of G''. The XRD patterns and DSC curves suggest that the compounds exhibit the smectic-A or -C* phase. G' and G'' increased again by almost 100-fold after the second transition, and $G' \approx 10 \times G''$ when **a6**, **b6**, and **c6** further cooled, clearly indicating that they became solids. $G' \approx 100$ MPa, which is larger than G' for pressure-sensitive adhesives[56] but smaller than those for typical epoxy resins.[57] The changes in G' and G'' accompanying the thermal phase transitions of **a6**, **b6**, and **c6** were clearly distinguishable. That accompanying the thermal phase transition of **d6**, however, was ambiguous. G' and G'' continuously increased without plateauing between the first and second transitions of **d6**. The ambiguous change corresponds to the XRD pattern for **d6** in which the smectic-A and -B phases have clearly not separated.

The dynamic viscoelasticities of **a6**, **b6**, **c6**, and **d6** were measured while irradiating the compounds with UV and visible light at 25 °C to investigate the photochemical and isothermal transitions. G' and G'' for all the samples immediately decreased when the compounds were initially irradiated (Figure 5). Further irradiating **a6**, **b6**, and **c6** decreased G' to less than

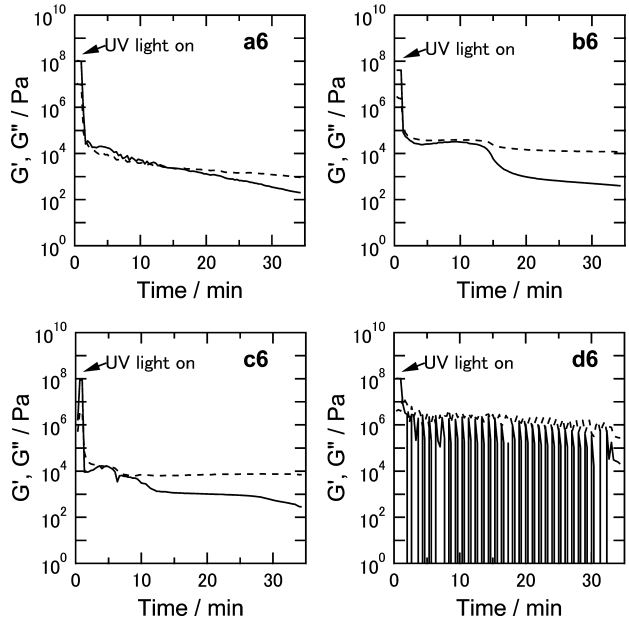

Figure 5. Dependence of storage modulus, G' (solid line), and loss modulus, G'' (dashed line), of **a6**, **b6**, **c6**, and **d6** on irradiation time at 30 °C.

one-tenth of G'', clearly suggesting that these solids transformed into liquids when irradiated with UV light but not heated. However, G'' remained >100, much higher than G'' for the molten samples. The irradiated sampleswere set out and visually inspected. The areas of the samples opposite the incident direction of the irradiation light had remained solid. Hence, the G' and G'' estimated for the photoliquefied samples must be considerably larger than the ideal G' and G'' for completely liquefied ones because the samples were heterogeneous. Thus, the values of G' and G'' are quantitatively invalid, but the drastic decrease in these values after photoirradiation can be induced by the local phase transition. Continuous irradiation of**d6**, on the other hand, did not further decrease G' and G'' but caused them both to fluctuate between 10^5 and 10^7. The whole-irradiated **d6** sample remained solid; thus, G' and G'' may have fluctuated because the sample and the stage were detached from each other at the interface, representing an alternating sliding frictional force.

Photocontrol of Adhesion. The possibility of applying **a6** to adhesives has already been studied.[15] A 0.7−1-μm-thick layer of thermally fused **a6** was sandwiched between two glass slides and cooled to room temperature to bond the slides together. The preliminary pulling test, in which the slides were manually separated, revealed that the adhesion was controllable at 50 and 0 N cm^{-2}, depending on the wavelength of the irradiation light.[15] For more accurate adhesion measurement, we carried out tensile lap-shear adhesive strength test using a material testing machine. Measurement was conducted for **a6**, **b6**, **c6**,

dx.doi.org/10.1021/am501227y | ACS Appl. Mater. Interfaces 2014, 6, 7933−7941

and **d6** before and after irradiation with 365 nm-light (80 mW cm^{-2}, 3 min) and 525 nm-light (25 mW^{-2},1.5 min), respectively. If glass slides are gripped directly by holding apparatus (chucks), fracture will occur near the chucks before adhesive peeling because glass is brittle material. It is the same in the case of using aluminum tabs. In addition, because glass slides have high torsional rigidity for adhesive strength in this experiment, torsion will lead to the separation of glass slides, even though it is very slight. Thus, a 0.4 mm-thick stainless-steel sheet was connected to glass at the end of the slides. And the thin stainless sheets were gripped by chucks. Thereby unexpected fracture and torsion were suppressed, and reliable data were obtained. Stress−strain curves were measured three times for each condition. Figure 6 represents only the typical

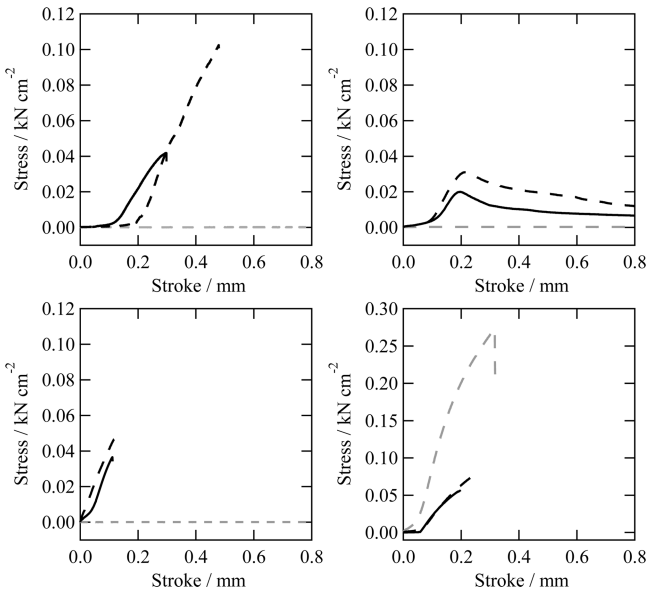

Figure 6. Stress and strain curves of (a) **a6**, (b) **b6**, (c) **c6**, and (d) **d6** before irradiation (solid line) and after irradiation with 365 nm-light (gray dashed line) and subsequent irradiation with 525 nm-light (dashed line).

curves. Alternatively, for the certification of reproducibility, the averaged values of critical stress were listed with standard deviations in Table 4.

Table 4. Adhesion Strength of Azobenezenes before and after Irradiation with Light

	adhesion strength (N cm^{-2})		
	before irradiation	365 nm-light	525 nm-light
a6	42.4 ± 1.1	0.2	100.4 ± 5.6
b6	18.8 ± 1.7	0.3	30.2 ± 0.9
c6	46.8 ± 7.1	0.1	53.8 ± 10.2
d6	64.9 ± 8.0	274.4 ± 1.5	80.5 ± 10.4

Accordingly, the adhesion strength of the nonirradiated **a6** was measured as 40 N cm^{-2}, which was comparable to that of conventional double-stick tape. The adhesion force then decreased to 0 N cm^{-2} when the **a6** was irradiated with UV light, irrespective of the magnitude of the applied strain. No magnitude of stress applied under any stroke will cause adhesives to fluidize. In other words, the two glass slides smoothly slid because they were separated by a liquid layer. The two glass slides were restacked and irradiated with visible light, causing them to refix. Interestingly, the adhesion strength increased to 100 N cm^{-2}, which is two-and-a-half times as large as that of the nonirradiated **a6** (40 N cm^{-2}). Two possible factors contribute to the increased adhesion. One is the cis-isomer effect. Irradiating **a6** with visible (525 nm) light produces a small amount of cis isomer (2.7%), which are more polar than trans isomer because the bent structure imparts a dipole moment to the cis isomers. Thus, the additional interaction between the polar components and the polar glass surface could strengthen the adhesion. The other is the change in the mechanical characteristics of the adhesives. The solids isothermally generated by photoisomerizing isotropic liquids could be different from thermally generated solids. POM observation revealed that the domains in the photochemically-generated solid were very small, which might increase the mechanical strength of the solid, and were darker than those in the thermally generated one.

The adhesion strength values of the non-, UV-, and UV−visible-irradiated **c6** were 47, 0, and 57 N cm^{-2}, respectively. The adhesions of the UV−visible-irradiated one were only slightly stronger than those of the nonirradiated samples. It is in contrast to the drastic increase of adhesion strength of **a6** after visible-irradiation. Although we need further investigation to understand the reason for the photoenhancement of the adhesion strength, at least we identify that **c6** can be used as a reworkable adhesive, as well as **a6**.

The adhesion strength values of the non-, UV-, and UV−visible-irradiated **b6** were 19, 0, and 30 N cm^{-2}, respectively. The adhesion of the nonirradiated **b6** increased with increasing stroke to a maximum (19 N cm^{-2}) and then decreased with decreasing adhered surface area without the glass slides separating. The adhesive layer remained on one glass surface and slid at the other during the measurements, meaning that the thin adhesive layer at the sliding surface continuously deformed and acted as a viscous layer under applied shear stress. The irradiation on the **b6** with UV light decreased its adhesion strength to 0 N cm^{-2}, and then irradiating with visible light recovered the strength to 30 N cm^{-2}. After irradiation with visible light, the two glass plates were continuously refixed under the maximum shear stress. The **b6** may have shown continuous adhesion beyond the maximum shear stress because it is thixotropic, which may owe to its softness. The elastic moduli for solid **b6** were half as large as those for solid **a6** and **c6**, indicating that the **b6** was softer than the **a6** and **c6**. In addition, noncrystalline **b6** that does not undergo glass transition is neither a crystalline solid nor a glassy one but consists of liquid crystals (smectic-F/I) at room temperature, although it was considered solid on the basis of its viscoelasticity (i.e., $G' > G''$), which may also possibly explain its low adhesion (19 N cm^{-2}) as a "solid".

The adhesion strength values of **a6**, **b6**, and **c6** decreased to 0 N cm^{-2} when the adhesives were irradiated with UV light during the pulling test, indicating that the adhesives photochemically transitioned to liquids. The **d6**, which did not show a photochemical phase transition, showed unique adhesion. The adhesion strength values of the non-, UV-, and UV−visible-irradiated **d6** were 65, 270, and 81 N cm^{-2}, respectively. The adhesion of the nonirradiated **d6** is comparable to those of the nonirradiated **a6**, **b6**, and **c6**, but it drastically increased by 1 order of magnitude to 270 N cm^{-2} when the **d6** was irradiated with UV light. The increased adhesion is comparable to that of conventional adhesives. We, therefore, decreased the

adhesive area to one-third of the initial one for the pulling test of **d6**, because otherwise the too strong applied shear stress broke the glass slides before separating from each other. The cis-rich **d6** was solid, it could be used as an adhesive even after being irradiated with UV light, and it exhibited somewhat stronger adhesion than the **a6**, **b6**, and **c6** because of its polar cis isomers generated when it was irradiated with UV light. The polar components in adhesives can interact strongly with the surface of glass plates, and enhance the adhesion force if the adhesive is robust enough to surpass cohesive failure.The **d6** irradiated with visible light showed an adhesion strength of 84 N cm^{-2}. Contrary to the adhesions of the **a6**, **b6**, and **c6**, that of the **d6** increased when the **d6** was irradiated with UV light and decreased when it was irradiated with visible light. Inconveniently, either a solvent must be used or the **d6** must be heated to liquefy the **d6** so that it adheres to surfaces because irradiation with light cannot liquefy it. The cis isomers in the **d6** gradually transform into trans ones over a few days even at room temperature. The stronger adhesion of the **d6** can only be maintained for a limited time. Hence, **d6** can act as a suitable adhesive when strong adhesion is temporarily required. The enhancement of adhesion on irradiation with UV-light should be repeatable. Actually the isomerization of **d6** in a film was repeatable as well as those of the other compounds. Thus, the term of strong temporal adhesion can be prolonged by additional irradiation with UV-light.

CONCLUSIONS

One of novel sugar-alcohol derivatives with multiazobenzene arms was reversibly liquefied and solidified when irradiated with UV and visible light. The dynamic viscoelasticity measurement revealed continuous liquid crystalline transition of **d6**. We previously reported that at least four or more azobenzene arms were necessary to photoinduce the phase transition because neither solid mono- nor solid diazobenzene photoisomerized when they were irradiated with UV light. Thus, the first requirement for photoinduced phase transition is that photoisomerization occurs in a solid state. All the hexamers underwent solid-state isomerization independent of the number of tails, spacers, and sugar-alcohol scaffolds they contained; however, the different structures affected the phase transition behaviors. Concretely, the mannitol derivatives prepared without alkyl tails and with decamethylene spacers and the compounds prepared with hexyl tails exhibited photoinduced phase transitions, but the compounds prepared without alkyl tails and with pentamethylene spacers did not. In addition, the other hexamer prepared with a cyclic scaffold did not transform into liquid when it was irradiated with light. Thus, the second requirement for photoinduced phase transition at room temperature is that the solid−liquid transition temperatures of cis- and trans-isomers should be below and above room temperature, respectively. Consequently, only the liquid crystalline compounds exhibited photochemical phase transitions.

The adhesions of the compounds were tuned by alternately irradiating the compounds with UV and visible light. The adhesions of the compounds that underwent photochemical phase transitions decreased to almost 0 N cm^{-2} when the compounds were irradiated with UV light and increased when they were irradiated with visible light. Irradiating the compounds with visible light resolidified them, increasing their adhesion, suggesting they work as suitable adhesives. In contrast, **d6** showed weaker adhesion when irradiated with visible light and stronger adhesion when irradiated with UV light. The materials that did not undergo photoinduced phase transitions showed a different mode for adjusting adhesion. The maximum adhesion was ∼300 N cm^{-2}, which is comparable to conventional adhesives.

EXPERIMENTAL PROCEDURES

Materials. The chemical compounds used herein are shown in Figure 1. We previously described the synthesis of methyl 4-(4-hexylphenylazo)phenoxy-11-undecanoate (**a1**), ethylene bis[4-(4-hexylphenylazo)phenoxy-11-undecanoate] (**a2**), tetrakis-*O*-[4-(4-hexylphenylazo)phenoxyalkyl-11-undecanoyl]-L-threitol (**a4**), hexakis-*O*-[4-(4-hexylphenylazo)phenoxy-11-undecanoyl]-D-mannitol (**a6**), octakis-*O*-[4-(4-hexylphenylazo)phenoxy-11-undecanoyl]-1,1′-oxybis-(1-deoxyxylitol) (**a8**), hexakis-*O*-[4-(4-hexylphenylazo)phenoxy-11-undecanoyl]-*scyllo*-inositol (**aC6**), and hexakis-*O*-[4-(4-hexylphenylazo)phenoxy-6-hexanoyl]-d-mannitol (**b6**). Herein, we synthesized hexakis-*O*-[4-(phenylazo)phenoxy-11-undecanoyl]-D-mannitol (**c6**) and hexakis-*O*-[4-(phenylazo)phenoxy-6-hexanoyl]-D-mannitol (**d6**) from hydroxyl azobenzene through etherification with bromoalkanoic acid, the formation of acid chloride, and esterification with sugar alcohol. (The synthesis details are described in the Supporting Information).

Physical Measurements. DSC was conducted in a Seiko Instrument EXTAR 6000 calorimeter. The samples were irradiated using high-power light-emitting diodes [Nichia NC4U133A for UV (365 nm) light at 40−80 mW cm^{-2} and Luxeon LXHL-LM5C for visible (525 nm) light at 25 mW cm^{-2}]. The sample textures were observed using an optical microscope (Olympus BH2) equipped with a temperature controller (Mettler FP90) and a heat stage (Mettler FP82HT). The pictures and videos of the samples were taken using a video recorder (Sony Handycam HDR-CX170) with an ultramacrolens (Raynox MSN-505). The absorption spectra were measured using a Hewlett-Packard ultraviolet−visible (UV−vis) spectrophotometer (Agilent 8453). We prepared 4 wt % solutions by dissolving the samples in chloroform (Wako HPLC grade) and added polystyrene to each solution at the polystyrene/sample weight ratio of 1/20. The solutions were used to spin coat thin films onto 20 × 20 mm glass slides. The sample dynamic viscoelasticities were measured using an Anton Paar MCR 302 rheometer with a photoirradiation unit, Hamamatsu Photonics LC8, operated at 1 Hz. The sample thickness and diameter were 100 μm and 12 mm. The storage and loss elastic moduli were measured for the samples cooled from their isotropic phases at 3 °C min^{-1} to analyze the thermal phase transitions. The stress was continuously maintained at 30% for the isotropic liquids, varied in the range 30−0.1% between the first and second transitions, and varied in the range 0.1−0.01% after the second transition. The samples were maintained at 30 °C and the stress was varied in the range 0.01−30% when they were irradiated with UV light (700 mW cm^{-2}, 300−450 nm) to analyze the photoinduced phase transitions. The tensile shear strengths were measured three times using a Shimadzu Autograph tensile-testing machine with a 1-kN load cell, SLBL-1kN, and a holding apparatus, SCG-1kNA. Two 1.5 cm × 5 cm, 1 mm-thick glass slides connected to 0.2 mm-thick stainless-steel plates were bonded together by spreading 2−3 mg of the adhesives over a 1.5 cm × 1.5 cm area of the slides and pressing the slides together. The glass slides were pulled in opposite directions at 0.2 mm min^{-1}, and the stress was monitored during separation with the tensile-testing machine. Adhesion forces were determined as average values for three times measurement. Stable conformations of the compounds were calculated based on molecular mechanics and the molecular orbital method in Chem3D Ultra, and the molecular lengths were then determined for the structures. Liquid crystalline cells rubbed with polyimide (EHC KSOR-05) were used to identify the homogeneously aligned liquid crystalline phase. The two glass slides for a liquid crystalline cell were conventionally treated with octadecylsilane to homeotropically align the liquid crystalline phase.

■ ASSOCIATED CONTENT

Supporting Information

Synthesis details for the materials (**c6**, **d6**, and each intermediated compound), and the polaring optical micrographs, XRD patterns and differential scanning calorimetric curves for the materials (**a4**, **a6**, **a8**, **b6**, **c6**, and **d6**), and the estimation procedure for isomer ratios. This material is available free of charge via the Internet at http://pubs.acs.org/

■ AUTHOR INFORMATION

Corresponding Author

*E-mail: h.akiyama@aist.go.jp.

Author Contributions

The manuscript was written through contributions of all authors. All authors have given approval to the final version of the manuscript. S.K., Y.O., M.Y., H.K., H.N., Y.N., and R.A. contributed equally.

Notes

The authors declare no competing financial interest.

■ ACKNOWLEDGMENTS

This work was supported in part by the Grant for Basic Science Research Projects from the Sumitomo Foundation. The authors thank Anton Paar Japan for dynamic viscoelasticity measurement.

■ ABBREVIATIONS

UV = ultraviolet
G' = storage elastic modulus
G'' = loss elastic modulus
DSC = differential scanning calorimetry
POM = polarized optical microscopy
XRD = X-ray diffractometry

■ REFERENCES

(1) Boyne, J. M.; Millan, E. J.; Webster, I. Peeling Performance of a Novel Light Switchable Pressure-Sensitive Adhesive. *Int. J. Adhes. Adhes.* **2001**, *21*, 49−53.

(2) Gurney, R. S.; Dupin, D.; Nunes, J. S.; Ouzineb, K.; Siband, E.; Asua, J. M.; Armes, S. P.; Keddie, J. L. Switching Off the Tackiness of a Nanocomposite Adhesive in 30 s via Infrared Sintering. *ACS Appl. Mater. Interfaces* **2012**, *4*, 5442−5452.

(3) Inui, T.; Sato, E.; Matsumoto, A. Pressure-Sensitive Adhesion System Using Acrylate Block Copolymers in Response to Photoirradiation and Postbaking as the Dual External Stimuli for On-Demand Dismantling. *ACS Appl. Mater. Interfaces* **2012**, *4*, 2124−2132.

(4) Inui, T.; Yamanishi, K.; Sato, E.; Matsumoto, A. Organotellurium-Mediated Living Radical Polymerization (TERP) of Acrylates Using Ditelluride Compounds and Binary Azo Initiators for the Synthesis of High-Performance Adhesive Block Copolymers for On-Demand Dismantlable Adhesion. *Macromolecules* **2013**, *46*, 8111−8120.

(5) Ishikawa, H.; Seto, K.; Shimotuma, S.; Kishi, N.; Sato, C. Bond Strength and Disbonding Behavior of Elastomer and Emulsion-Type Dismantlable Adhesives Used for Building Materials. *Int. J. Adhes. Adhes.* **2005**, *25*, 193−199.

(6) June, S. M.; Suga, T.; Heath, W. H.; Lin, Q.; Puligadda, R.; Yan, L.; Dillard, D.; Long, T. E. Photoactive Polyesters Containing *o*-Nitro Benzyl Ester Functionality for Photodeactivatable Adhesion. *J. Adhes.* **2013**, *89*, 548−558.

(7) Kamperman, M.; Synytska, A. Switchable Adhesion by Chemical Functionality and Topography. *J. Mater. Chem.* **2012**, *22*, 19390−19401.

(8) Kim, D.; Chung, I.; Kim, G. Dismantlement Studies of Dismantlable Polyurethane Adhesive by Controlling Thermal Property. *J. Adhes. Sci. Technol.* **2012**, *26*, 2571−2589.

(9) Nishiyama, Y.; Uto, N.; Sato, C.; Sakurai, H. Dismantlement Behavior and Strength of Dismantlable Adhesive Including Thermally Expansive Particles. *Int. J. Adhes. Adhes.* **2003**, *23*, 377−382.

(10) Phillips, J. P.; Deng, X.; Stephen, R. R.; Fortenberry, E. L.; Todd, M. L.; McClusky, D. M.; Stevenson, S.; Misra, R.; Morgan, S.; Long, T. E. Nano- and Bulk-Tack Adhesive Properties of Stimuli-Responsive, Fullerene-Polymer Blends, Containing Polystyrene-block-Polybutadiene-block-Polystyrene and Polystyrene-block-Polyisoprene-block-Polystyrene Rubber-Based Adhesives. *Polymer* **2007**, *48*, 6773−6781.

(11) Sato, E.; Hagihara, T.; Matsumoto, A. Facile Synthesis of Main-Chain Degradable Block Copolymers for Performance Enhanced Dismantlable Adhesion. *ACS Appl. Mater. Interfaces* **2012**, *4*, 2057−2064.

(12) Sato, E.; Tamura, H.; Matsumoto, A. Cohesive Force Change Induced by Polyperoxide Degradation for Application to Dismantable Adhesion. *ACS Appl. Mater. Interfaces* **2010**, *2*, 2594−2601.

(13) Trenor, S. R.; Long, T. E.; Love, B. J. Development of a Light-Deactivatable PSA via Photodimerization. *J. Adhes.* **2005**, *81*, 213−229.

(14) Yamanishi, K.; Sato, E.; Matsumoto, A. Precise Synthesis of Acrylic Block Copolymers and Application to On-Demand Dismantlable Adhesion Systems in Response to Photoirradiation and Postbaking. *J. Photopolym. Sci. Technol.* **2013**, *26*, 239−244.

(15) Akiyama, H.; Yoshida, M. Photochemically Reversible Liquefaction and Solidification of Single Compounds Based on a Sugar Alcohol Scaffold with Multi Azo-Arms. *Adv. Mater.* **2012**, *24*, 2353−2356.

(16) Ikeda, T.; Horiuchi, S.; Karanjit, D. B.; Kurihara, S.; Tazuke, S. Photochemically Induced Isothermal Phase-Transition in Polymer Liquid-Crystals with Mesogenic Phenyl Benzoate Side-Chains 0.1. Calorimetric Studies and Order Parameters. *Macromolecules* **1990**, *23*, 36−42.

(17) Ikeda, T.; Horiuchi, S.; Karanjit, D. B.; Kurihara, S.; Tazuke, S. Photochemically Induced Isothermal Phase-Transition in Polymer Liquid-Crystals with Mesogenic Phenyl Benzoate Side-Chains 0.2. Photochemically Induced Isothermal Phase-Transition Behaviors. *Macromolecules* **1990**, *23*, 42−48.

(18) Ikeda, T.; Tsutsumi, O. Optical Switching and Image Storage by Means of Azobenzene Liquid-Crystal Films. *Science* **1995**, *268*, 1873−1875.

(19) Tazuke, S.; Kurihara, S.; Ikeda, T. Amplified Image Recording in Liquid-Crystal Media by Means of Photochemically Triggered Phase-Transition. *Chem. Lett.* **1987**, 911−914.

(20) Seki, T.; Sekizawa, H.; Ichimura, K. Morphological Changes in Monolayer of a Photosensitive Polymer Observed by Brewster Angle Microscopy. *Polymer* **1997**, *38*, 725−728.

(21) Seki, T.; Tamaki, T. Photomechanical Effect in Monolayers of Azobenzene Side-Chain Polymers. *Chem. Lett.* **1993**, 1739−1742.

(22) Alvarez-Lorenzo, C.; Deshmukh, S.; Bromberg, L.; Hatton, T. A.; Sandez-Macho, I.; Concheiro, A. Temperature- and Light-Responsive Blends of Pluronic F127 and Poly(*N*,*N*-Dimethylacrylamide-*co*-Methacryloyloxyazobenzene). *Langmuir* **2007**, *23*, 11475−11481.

(23) Chen, D.; Liu, H.; Kobayashi, T.; Yu, H. F. Multiresponsive Reversible Gels Based on a Carboxylic Azo Polymer. *J. Mater. Chem.* **2010**, *20*, 3610−3614.

(24) Duan, P. F.; Li, Y. G.; Li, L. C.; Deng, J. G.; Liu, M. H. Multiresponsive Chiroptical Switch of an Azobenzene-Containing Lipid: Solvent, Temperature, and Photoregulated Supramolecular Chirality. *J. Phys. Chem. B* **2011**, *115*, 3322−3329.

(25) Irie, M.; Iga, R. Photoresponsive Polymers 0.9. Photostimulated Reversible Sol-Gel Transition of Polystyrene with Pendant Azobenzene Groups in Carbon-Disulfide. *Macromolecules* **1986**, *19*, 2480−2484.

(26) Kim, J. H.; Seo, M.; Kim, Y. J.; Kim, S. Y. Rapid and Reversible Gel−Sol Transition of Self-Assembled Gels Induced by Photo-

isomerization of Dendritic Azobenzenes. *Langmuir* **2009**, *25*, 1761−1766.
(27) Kobayashi, H.; Koumoto, K.; Jung, J. H.; Shinkai, S. Sol−Gel Phase Transition Induced by Fiber-Vesicle Structural Changes in Sugar-Based Bolaamphiphiles. *J. Chem. Soc., Perkin Trans. 2* **2002**, 1930−1936.
(28) Kume, S.; Kuroiwa, K.; Kimizuka, N. Photoresponsive Molecular Wires of Fe-II Triazole Complexes in Organic Media and Light-Induced Morphological Transformations. *Chem. Commun.* **2006**, 2442−2444.
(29) Lee, S.; Kang, H. S.; Park, J. K. Directional Photofluidization Lithography: Micro/Nanostructural Evolution by Photofluidic Motions of Azobenzene Materials. *Adv. Mater.* **2012**, *24*, 2069−2103.
(30) Liao, X. J.; Chen, G. S.; Liu, X. X.; Chen, W. X.; Chen, F.; Jiang, M. Photoresponsive Pseudopolyrotaxane Hydrogels Based on Competition of Host−Guest Interactions. *Angew. Chem., Int. Ed.* **2010**, *49*, 4409−4413.
(31) Liu, Z. X.; Feng, Y.; Yan, Z. C.; He, Y. M.; Liu, C. Y.; Fan, Q. H. Multistimuli Responsive Dendritic Organogels Based on Azobenzene-Containing Poly(Aryl Ether) Dendron. *Chem. Mater.* **2012**, *24*, 3751−3757.
(32) Mamiya, J.; Kanie, K.; Hiyama, T.; Ikeda, T.; Kato, T. A Rodlike Organogelator: Fibrous Aggregation of Azobenzene Derivatives with a Syn-Chiral Carbonate Moiety. *Chem. Commun.* **2002**, 1870−1871.
(33) Matsuzawa, Y.; Ueki, K.; Yoshida, M.; Tamaoki, N.; Nakamura, T.; Sakai, H.; Abe, M. Assembly and Photoinduced Organization of Mono- and Oligopeptide Molecules Containing an Azobenzene Moiety. *Adv. Funct. Mater.* **2007**, *17*, 1507−1514.
(34) Murata, K.; Aoki, M.; Suzuki, T.; Harada, T.; Kawabata, H.; Komori, T.; Ohseto, F.; Ueda, K.; Shinkai, S. Thermal and Light Control of The Sol−Gel Phase-Transition in Cholesterol-Based Organic Gels—Novel Helical Aggregation Modes as Detected by Circular-Dichroism and Electron-Microscopic Observation. *J. Am. Chem. Soc.* **1994**, *116*, 6664−6676.
(35) Peng, K.; Tomatsu, I.; Kros, A. Light Controlled Protein Release from a Supramolecular Hydrogel. *Chem. Commun.* **2010**, *46*, 4094−4096.
(36) Rajaganesh, R.; Gopal, A.; Das, T. M.; Ajayaghosh, A. Synthesis and Properties of Amphiphilic Photoresponsive Gelators for Aromatic Solvents. *Org. Lett.* **2012**, *14*, 748−751.
(37) Wang, C.; Chen, Q.; Sun, F.; Zhang, D. Q.; Zhang, G. X.; Huang, Y. Y.; Zhao, R.; Zhu, D. B. Multistimuli Responsive Organogels Based on a New Gelator Featuring Tetrathiafulvalene and Azobenzene Groups: Reversible Tuning of the Gel−Sol Transition by Redox Reactions and Light Irradiation. *J. Am. Chem. Soc.* **2010**, *132*, 3092−3096.
(38) Wu, Y. P.; Wu, S.; Tian, X. J.; Wang, X.; Wu, W. X.; Zou, G.; Zhang, Q. J. Photoinduced Reversible Gel-Sol Transitions of Dicholesterol-Linked Azobenzene Derivatives Through Breaking and Reforming of Van Der Waals Interactions. *Soft Matter* **2011**, *7*, 716−721.
(39) Yagai, S.; Iwashima, T.; Kishikawa, K.; Nakahara, S.; Karatsu, T.; Kitamura, A. Photoresponsive Self-Assembly and Self-Organization of Hydrogen-Bonded Supramolecular Tapes. *Chem.—Eur. J.* **2006**, *12*, 3984−3994.
(40) Yagai, S.; Karatsu, T.; Kitamura, A. Melamine-Barbiturate/Cyanurate Binary Organogels Possessing Rigid Azobenzene-Tether Moiety. *Langmuir* **2005**, *21*, 11048−11052.
(41) Zhao, Y. L.; Stoddart, J. F. Azobenzene-Based Light-Responsive Hydrogel System. *Langmuir* **2009**, *25*, 8442−8446.
(42) Karageorgiev, P.; Neher, D.; Schulz, B.; Stiller, B.; Pietsch, U.; Giersig, M.; Brehmer, L. From Anisotropic Photo-Fluidity towards Nanomanipulation in The Optical Near-Field. *Nat. Mater.* **2005**, *4*, 699−703.
(43) Lee, S.; Kang, H. S.; Park, J. K. Directional Photofluidization Lithography: Micro/Nanostructural Evolution by Photofluidic Motions of Azobenzene Materials. *Adv. Mater.* **2012**, *24*, 2069−2103.
(44) Kim, D. Y.; Tripathy, S. K.; Li, L.; Kumar, J. Laser-Induced Holographic Surface-Relief Gratings on Nonlinear-Optical Polymer-Films. *Appl. Phys. Lett.* **1995**, *66*, 1166−1168.
(45) Rochon, P.; Batalla, E.; Natansohn, A. Optically Induced Surface Gratings on Azoaromatic Polymer-Films. *Appl. Phys. Lett.* **1995**, *66*, 136−138.
(46) Ichimura, K. Reversible Photoisomerisability and Particle Size Changes of Mill-Dispersed Azobenzene Crystals in Water. *Chem. Commun.* **2009**, 1496−1498.
(47) Koshima, H.; Ojima, N.; Uchimoto, H. Mechanical Motion of Azobenzene Crystals upon Photoirradiation. *J. Am. Chem. Soc.* **2009**, *131*, 6890−+.
(48) Nakayama, K.; Jiang, L.; Iyoda, T.; Hashimoto, K.; Fujishima, A. Photo-Induced Structural Transformation on The Surface of Azobenzene Crystals. *Jpn. J. Appl. Phys., Part 1* **1997**, *36*, 3898−3902.
(49) Uchida, K.; Izumi, N.; Sukata, S.; Kojima, Y.; Nakamura, S.; Irie, M. Photoinduced Reversible Formation of Microfibrils on a Photochromic Diarylethene Microcrystalline Surface. *Angew. Chem., Inter. Ed.* **2006**, *45*, 6470−6473.
(50) Uchida, K.; Nishikawa, N.; Izumi, N.; Yamazoe, S.; Mayama, H.; Kojima, Y.; Yokojima, S.; Nakamura, S.; Tsujii, K.; Irie, M. Phototunable Diarylethene Microcrystalline Surfaces: Lotus and Petal Effects upon Wetting. *Angew. Chem., Inter. Ed.* **2010**, *49*, 5942−5944.
(51) Norikane, Y.; Hirai, Y.; Yoshida, M. Photoinduced Isothermal Phase Transitions of Liquid-Crystalline Macrocyclic Azobenzenes. *Chem. Commun.* **2011**, *47*, 1770−1772.
(52) Uchida, E.; Sakaki, K.; Nakamura, Y.; Azumi, R.; Hirai, Y.; Akiyama, H.; Yoshida, M.; Norikane, Y. Control of the Orientation and Photoinduced Phase Transitions of Macrocyclic Azobenzene. *Chem.—Eur. J.* **2013**, *19*, 17391−17397.
(53) Okui, Y.; Han, M. N. Rational Design of Light-Directed Dynamic Spheres. *Chem. Commun.* **2012**, *48*, 11763−11765.
(54) Akiyama, H.; Tanaka, A.; Hiramatsu, H.; Nagasawa, J.; Tamaoki, N. Reflection Colour Changes in Cholesteric Liquid Crystals after the Addition and Photochemical Isomerization of Mesogenic Azobenzenes Tethered to Sugar Alcohols. *J. Mater. Chem.* **2009**, *19*, 5956−5963.
(55) Victor, J. G.; Torkelson, J. M. On Measuring the Distribution of Local Free Volume in Glassy Polymers by Photochromic and Fluorescence Techniques. *Macromolecules* **1987**, *20*, 2241−2250.
(56) Benedek, I. *Pressure-Sensitive Adhesives and Applications*, 2nd revised and expanded ed.; Marcel Dekker Inc.: New York, 2004; Chapter 2−1, pp 5−35.
(57) Gupta, V. B.; Drzal, L. T.; Lee, C. Y. C.; Rich, M. J. The Effects of Stoichiometry and Structure on the Dynamic Torsional Properties of a Cured Epoxy-Resin System. *J. Macromol. Sci., Part B: Phys.* **1985**, *23*, 435−466.